KSCE Journal of Civil Engineering (2021) 25(10):4018-4031
DOI 10.1007/s12205-021-2104-4

pISSN 1226-7988, eISSN 1976-3808
www.springer.com/12205

Water Resources and Hydrologic Engineering

The Evaluation of the Hydrogeological Parameters of a Field Pumping Test within Multi-layer Unconfined Pebble Aquifers: A Case Study

Jianjun Ma[a], **Da Li**[a], **and Man Wang**[a]

[a]*School of Civil Engineering, Henan University of Science and Technology, Luoyang 471023, China*

ARTICLE HISTORY

Received 24 November 2020
Accepted 25 April 2021
Published Online 23 June 2021

KEYWORDS

Pumping test
Unconfined pebble aquifers
Hydraulic conductivity
Neuman model
Numerical simulation

ABSTRACT

This paper presents a case study of field pumping tests and the evaluation of the hydrogeological parameters of the unconfined pebble aquifers in the test site located at Shijiawan station in Luoyang City, China, which guarantees the construction safety of Metro Line 1. Multiple groups of single-well pumping tests and one group-well pumping test were conducted to obtain the aquifers' hydrogeological parameters. Then, a combination of theoretical analysis and numerical simulation was used to evaluate the aquifers' hydrogeological parameters. The analytical solutions were obtained for the unconfined, anisotropic pebble aquifers using the Neuman model. The numerical simulation was established via the finite element method (FEM). The calculation results indicate that the theoretical analysis and numerical simulation parameters are well matched. Moreover, the results of the numerical method which considers the heterogeneous and horizontal isotropic characteristics of the pebble stratum, as well as the hydrogeological parameters are more reliable than the results obtained by the theoretical analysis. The pumping tests also indicate that the supporting structure plays a significant role in waterproofing during dewatering construction.

1. Introduction

With the rapidly increasing development of urban construction and underground space in China, the safety of deep foundation pits has become a significant problem (Shen et al., 2015; Cao et al., 2019). A soil stratum consisting of large-thickness pebble layers is distributed in China's central regions, and is characterized by complex mechanical properties and a granular composition. The pebble strata are mostly characterized by high porosity and strong permeability. When excavating deep foundation pits in groundwater-rich areas, such as pebble aquifers, dewatering is a fundamental problem. Actual survey results have shown that the leakage or seepage damage of engineering construction in the water-rich pebble strata accounts for about 40% to 50% of total engineering accidents. Thus, the dewatering of deep foundation pits is the most effective means by which to prevent engineering accidents.

In the dewatering design of foundation pits, the accuracy of the aquifer's hydrogeological parameters plays a crucial role (Shaqour and Hasan, 2008; Zhang et al., 2020). Accordingly, hydraulic conductivity is an essential parameter in hydrogeological calculations (Chapuis et al., 2005; Yeh and Huang, 2009; Huang and Qian, 2012); the value of the aquifer's hydraulic conductivity has a direct effect on the estimation of the amount of foundation pit discharge, the control of formation settlement, and the evaluation of the environmental impact. Moreover, the hydraulic conductivity may also influence the selection and embedded depth of the supporting structure of the foundation pit. While there are many methods for the measurement of the hydrogeological parameters of aquifers, the most common ways to evaluate the hydraulic conductivity include predictive methods (Jiao, 1996; Chapuis, 2004), laboratory tests (Chapuis, 1992; Ma et al., 2014), and field tests (Jean, 1996; Ou and Chen, 2010). The most effective method is to calculate the hydrogeological parameters via field tests, such as pumping tests. Based on the data from pumping tests, the hydraulic conductivities of aquifers can be obtained by either analytical methods or numerical simulations that consider the relationship between the discharge and groundwater level (Çimen, 2008; Lin et al., 2010; Sethi, 2011; Kuang et al., 2014). However, analytical methods have certain limitations, and are only applicable to cases in which the geometric shapes and boundary conditions are homogeneous. Without a

CORRESPONDENCE Jianjun Ma majianjun@haust.edu.cn School of Civil Engineering, Henan University of Science and Technology, Luoyang 471023, China

systematic approach by which to determine the hydrogeological parameters of aquifers with complex field conditions, it is difficult to obtain accurate solutions via analytical methods (Neuman et al., 2007; Wu et al., 2008). With the development of digital calculation technology, back-calculation via a numerical approach has become widely used (Johnso et al., 2002). Compared with theoretical analysis, numerical simulation can more accurately yield the hydrogeological parameters of aquifers under complicated pumping test conditions. Previous research has shown that appropriate calculation models can be selected to obtain reliable hydrogeological parameters of aquifers via field pumping tests. Moreover, the regional characteristics of the hydrogeological parameters of unconfined pebble aquifers are significant, and their solution requires the use of a combination of both theoretical analysis and numerical simulation based on pumping test data.

This study presents a field case study of pumping tests in Luoyang, China. The pumping tests were carried out in the flood plain of the Luohe River to obtain the hydrogeological parameters of unconfined pebble aquifers. During the pumping tests, the related parameters of the pumping rate, drawdown, and discharge were measured. Then, the hydrogeological parameters were obtained via a combination of theoretical analysis and numerical simulation. Moreover, a three-dimensional finite element model was established to back-calculate the hydraulic conductivity values of the unconfined pebble aquifers. A two-well pumping test was also performed to verify the accuracy of the hydraulic conductivity.

2. Field Pumping Tests and Results

2.1 Site Conditions

The total length of Line No. 1 of the Luoyang Metro in China is 22.35 km. The bases of the station foundation pits, including the Youth Palace station to Yangwan station in the eastern section of the Luoyang Metro, are located in a loose to slightly dense pebble formation. Particular research work was conducted at Shijiawan station as a test section to ensure construction safety. In the field pumping test, the essential target was to calculate the hydrogeological parameters of the pebble aquifers in the flood plain of Luohe River. According to the geological survey report, the pebble formations within the construction site of Shijiawan station are unconfined aquifers.

Shijiawan station is located in the Chanhe district of Luoyang, and Fig. 1 presents the schematic diagram of the construction site of the station. As shown in Fig. 1, the station pit is located at the intersection of Anju Road and Zhongzhou East Road, and there are several high-rise residential structures around it. The station is an underground project with an estimated depth of 18 m, and its length and width are 203.35 m and 19.30 m, respectively. The project was constructed by the open-cut method, and the supporting structure of the foundation pit is a waterproof curtain composed of bored piles and plain concrete piles. During the field test, the pumping tests were carried out without the supporting structure. To reduce the effect of the pumping tests on the surrounding groundwater environment, the tests were performed at the eastern end of the foundation pit.

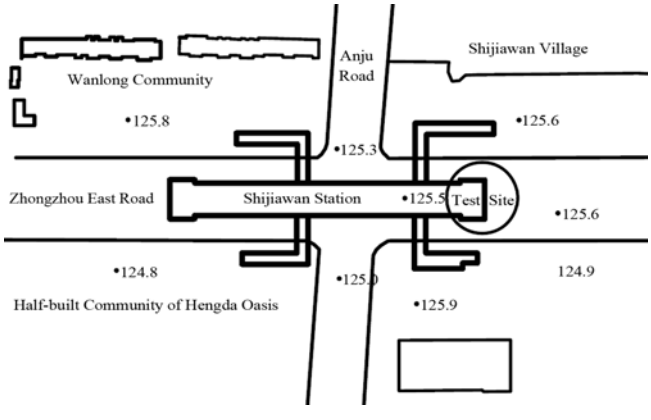

Fig. 1. The Schematic Diagram of the Construction Site of Shijiawan Station

2.2 Engineering Geology and Hydrogeology

2.2.1 Engineering Geology

The geomorphic unit is the flood plain of the Luohe River, in which the construction site is located. Fig. 2 shows the soil profile of the construction site. The elevation at the test site is 125.3 – 125.4 m above sea level. The figure also reveals that the stratum is composed of Holocene alluvial-diluvial beds and Upper Pleistocene alluvial-diluvial beds. The first layer is loess-like silt in the top 1.0 – 5.3 m below the ground surface, followed by fine sand to a depth of 0.7-5.0 m. The next layer is a pebble layer extending to a depth of 15.1 m, which is underlain by another pebble layer to a depth of more than 80 m.

The stratum parameters along the depth were established via laboratory tests. The grain size distribution indicates that the pebble content of the loose pebble strata is more than 50%. With the increase of the buried depth of the stratum, the pebble content increases significantly. The pebble content of the compacted pebble strata is relatively high, approximately 72%. Morevoer, the grain size of the pebble changes with the buried depth, and the variation range of the grain size is from 2 cm to more than 20 cm. Moreover, there are a small number of large boulders contained in the compacted pebble strata.

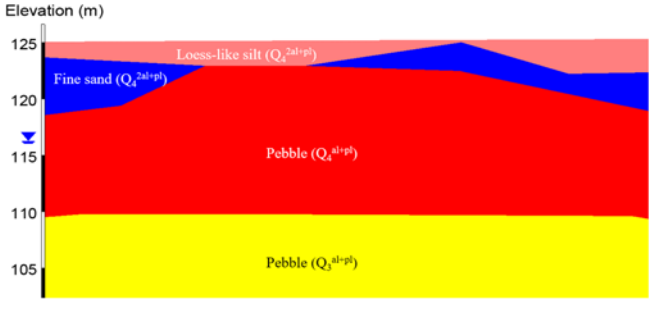

Fig. 2. The Soil Profile of the Construction Site

2.2.2 Hydrogeology

According to the buried conditions of aquifers, the type of groundwater is unconfined. The groundwater level was determined to be 116.71 – 116.90 m via site measurements during the exploration. The groundwater is mainly present in the loose to slightly dense pebble stratum of the Holocene series and the medium-dense to compacted pebble stratum of the Upper Pleistocene series. The hydrogeological characteristics of the unconfined aquifers are a large groundwater volume, medium water-abundance, and obvious water permeability. Local experiences and the results of laboratory tests revealed that the variation of the hydraulic conductivity values of the unconfined aquifers ranges from 60 to 160 m/d. The sources of groundwater recharge are atmospheric precipitation, canal water, irrigation water, and river water. The primary mode of groundwater drainage is artificial exploitation, followed by groundwater runoff.

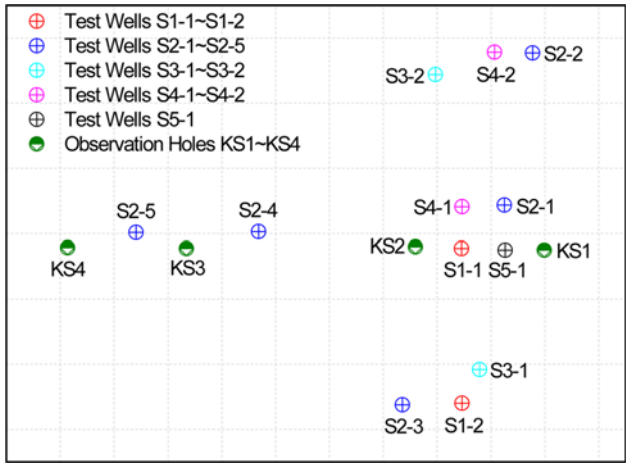

Fig. 3. The Plan View of the Pumping Test

2.3 Pumping Tests and Results

2.3.1 Pumping Tests

Pumping tests were carried out between February 19 and March 15, 2017 (the season was spring). Fig. 3 presents the plan view of the test wells and observation holes. There were five types of pumping wells (respectively labeled S1, S2, S3, S4, and S5) and four observation holes for the measurement of the pore water pressure (respectively labeled KS1, KS2, KS3, and KS4). During the pumping tests, the test wells all had the function of pumping and monitoring. For example, when well S2-5 was the pumping well, the other wells were the monitoring wells.

Table 1 lists the parameters of the test wells. During the pumping tests, the survey focus was on the hydrogeological

Table 1. The Parameters of the Test Wells

Type	Label	Depth (m)	Depth of well screen(m)	Diameter of well bore (mm)	Diameter of well tube (mm)	Depth of desilting tube (m)
1	S1-1 – S1-2	14.0	5.0 – 13.0	550	325	13.0 – 14.0
2	S2-1 – S2-5	24.0	15.0 – 23.0	550	325	23.0 – 24.0
3	S3-1 – S3-2	26.0	15.0 – 25.0	550	325	24.0 – 25.0
4	S4-1 – S4-2	30.0	24.0 – 29.0	550	325	29.0 – 30.0
5	S5-1	37.0	31.0 – 36.0	550	325	36.0 – 37.0

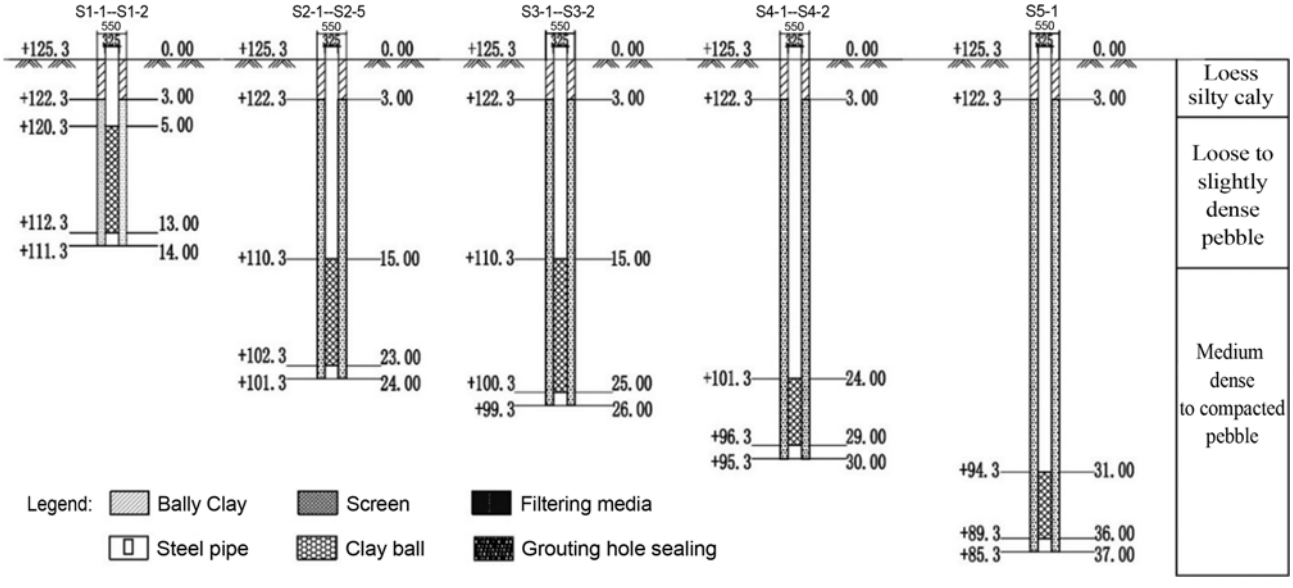

Fig. 4. The Structures of the Test Wells

parameters of the unconfined pebble aquifers. Fig. 4 presents the structure of the test wells, which were partially penetrating wells with an internal diameter of 325 mm and an external diameter of 550 mm. The filter tubes of the first and second types of test wells were 8.0 m long, those of the third type were 10.0 m long, and those of the fourth and fifth types were 5.0 m long. The filter tube of the first type of test well was located in the loose to slightly dense pebble stratum of the Holocene series, and was mainly used to measure the hydrogeological parameters of this unconfined pebble aquifer. The depths of the second and third types of test wells were the same as those of the dewatering well for dewatering construction in the foundation pit. The dewatering construction of the foundation pit can be determined by comparing the pumping effects of the wells with different structures.

The second and third types of test wells were used to measure the hydrogeological parameters of the medium-dense to compacted pebble stratum of the Upper Pleistocene series. The filter tube of the fourth type of well was installed in the range from the supporting structure to the bottom of the dewatering wells, and was used to measure the vertical hydraulic conductivity of the medium-dense to compacted pebble stratum. The filter tube of the fifth type well was installed in the lower part of the supporting structure, and was also used to measure the vertical hydraulic conductivity of the medium-dense to compacted pebble stratum.

To overcome the shortcomings of the pebble stratum, such as its poor self-stability and easy ability to collapse, drilling was carried out by a combination of impact drilling and mud protection based on local construction experience. Correspondingly, according to the design and the Chinese Construction Code related to dewatering (Standard for hydrogeological investigation of water-supply (GB50027-2001, 2001); Technical code for tube well (GB50296-2014, 2014)), the steel well pipes were welded and installed on site. Furthermore, the gap between the borehole and the well pipe was backfilled by gravel filter material. Two types of filter material were used in the pumping tests, the grain size of the first type was about 5 – 8 mm, while the grain size of the second type was about 7 – 10 mm. Finally, the wellhead was plugged and protected with cohesive soil.

Pumping tests were carried out without the effect of the supporting structure. Moreover, the initial groundwater levels of the test wells were measured before the pumping tests. The pumping tests consisted of two stages, namely the pumping stage and the recovery stage. During the pumping tests, submersible pumps with three different specifications were used for pumping, the flow rates of which were respectively 50, 20, and 30 m^3/h. An automated monitoring system with an accuracy of 1 cm was used to measure the groundwater levels of the test wells. The water discharges were measured by a flow meter, which had an accuracy of 0.1 m^3.

Table 2 reports the main data and processes of the pumping tests, which were carried out in two stages (with and without the supporting structure) to evaluate the impact of the supporting structure. In each tage, the pumping tests included both single-well and group-well pumping tests. The pumping period ranged from 720 to 10,080 min, and the recovery time was between 720 and 6,480 min. The drawdown of the pumping well was between 4.22 and 15.59 m, and the discharge rate of the pumping well was between 15.50 and 69.50 m^3/h.

2.3.2 Results of Pumping Tests without the Supporting Structure

2.3.2.1 Results of the Single-Well Pumping Tests

As shown in Table 2, four single-well pumping tests without the effect of the supporting structure were carried out, and the results are reported in Table 3. There were two drawdown scales in the

Table 2. The Main Data and Processes of the Pumping Tests

Case	Pumping well	Drawdown scale	h_0 (m)	s_w (m)	t_0	t_e	t_p (min)	t_r (min)	Q (m^3/h)
Without the supporting structure	S2-5	Large	8.15	13.82	19:00 21 Feb.	19:00 22 Feb.	1,440	/	69.50
		Small		4.22	19:00 22 Feb	19:00 23 Feb.	720	720	38.40
	S2-2	/	8.28	5.33	21:00 23 Feb	9:00 7 Mar.	10,080	6,480	20.90
	S2-3		8.12	13.93			10,080	6,480	36.60
	S3-1		8.10	15.59			10,080	6,480	33.30
	S3-2		8.10	15.22			10,080	6,480	35.30
	S1-2	/	7.70	4.79	21:00 7 Mar.	21:00 8 Mar.	720	720	15.85
	S3-2	/	8.10	11.22	21:00 8 Mar.	21:00 9 Mar.	720	720	36.20
	S4-2	/	8.13	11.84	20:00 11 Mar.	20:00 12 Mar.	720	720	15.50
With the supporting structure	S2-2	/	8.33	13.61	8:00 29 May	9:00 2 Jun.	4,320	1,440	21.89
	S2-3		8.49	9.26			4,320	1,440	21.98
	S3-1		8.37	7.37			4,320	1,440	39.30
	S3-2		8.30	11.83			4,320	1,440	36.05
	S2-4	/	8.24	13.11	9:00 2 Jun.	9:00 4 Jun.	720	720	26.00

Notes: h_0: the depth of static water head; s_w: the drawdown of pumping well; t_0: the start time of the pumping test; t_e: the end time of the pumping test; t_p and t_r: the lengths of the pumping stage and recovery stage, respectively; Q: the discharge of single pumping well.

Table 3. The Data for the Single-Well Pumping Tests

Pumping well	Monitoring well	Depth of well screen (m)	Distance from pumping well (m)	Drawdown (m)	
				Large	Small
S2-5	S2-1	15 – 23	34.25	0.190	0.114
	S2-2	15 – 23	39.09	0.240	0.105
	S2-3	15 – 23	27.55	0.250	0.110
	S2-4	15 – 23	11.30	0.400	0.201
	S2-5	15 – 23	/	13.822	4.220
S1-2	S1-1	5 – 13	11.10	0.04	
	S1-2	5 – 13	/	4.79	
S3-2	S3-1	15 – 25	21.49	0.28	
	S3-2	15 – 25	/	11.22	
S4-2	S4-1	24 – 29	11.60	0.49	
	S4-2	24 – 29	/	11.84	

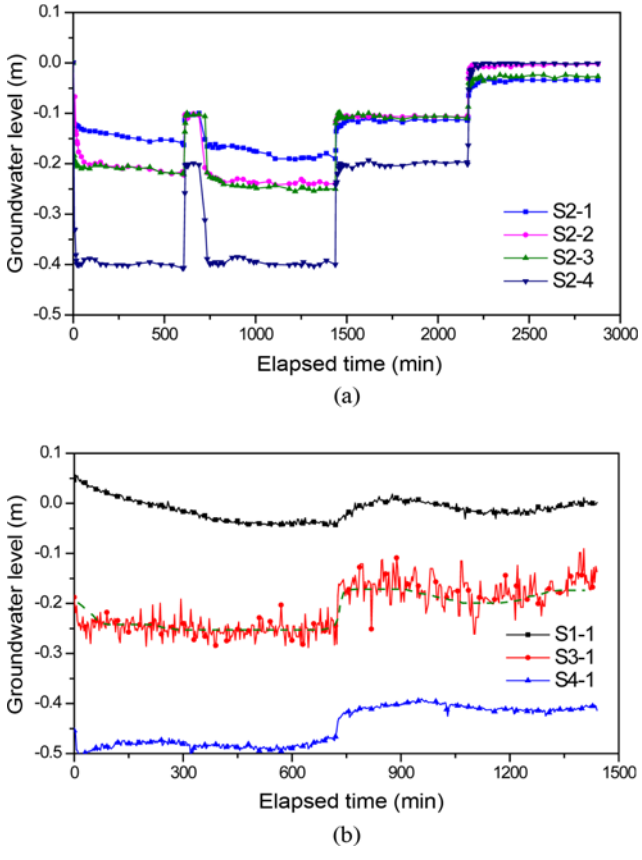

Fig. 5. The Variation of the Groundwater Level in the Monitoring Wells during the Single-Well Pumping Tests: (a) Pumping Well S2-5, (b) Pumping Wells S1-2/S3-2/S4-2

single-well pumping tests of S2-5.

Figure 5 presents the dynamic groundwater level in the monitoring wells during the single-well pumping tests. During the single-well pumping test of S2-5, the changes of the groundwater head followed similar trends. When the drawdown of the pumping well changed from large to small, the groundwater head rose rapidly and then reached a steady level. After the pump was shut down, the groundwater head recovered quickly. However, during the single-well pumping tests of S1-2, S3-2, and S4-2, the change trend of the groundwater head in each monitoring wells was complicated. Moreover, because the measured data for monitoring well S3-1 was unstable, the skeleton curve of the groundwater head is provided in the form of a chain dotted line. The discharge rates of S1-2 and S4-2 were both about 15.50 – 15.85 m^3/h, and the groundwater level of monitoring well S4-1 declined sharply, whereas the groundwater level of S1-1 was essentially unchanged.

Table 4. The Data of the Group-Well Pumping Test

Pumping well	Monitoring well	Depth of well screen (m)	Drawdown (m)
S2-2 S2-3 S3-2 S3-1	S1-1	5-13	0.87
	S1-2	5-13	1.23
	S2-1	15-23	0.84
	S2-4	15-23	0.73
	S2-5	15-23	0.66
	S4-1	24-29	1.10
	S4-2	24-29	0.73
	S5-1	31-36	0.34

2.3.2.2 Results of the Group-Well Pumping Test

S2-2, S2-3, S3-2, and S3-1 were selected as pumping wells for the group-well pumping test. As presented in Table 2, the pumping period was 10,080 min, the recovery time was 6,840 min, and the total discharge rate was about 126.1 m^3/h. Table 4 reports the results of the group-well pumping test. and Fig. 6 presents the groundwater level variation measured in the monitoring wells during the group-well pumping test.

As exhibited in Fig. 6, the changes in the groundwater head measured in the monitoring wells followed similar trends. The groundwater head initially declined rapidly over 6 min, after which it decreased at a slower rate until it reached a steady level.

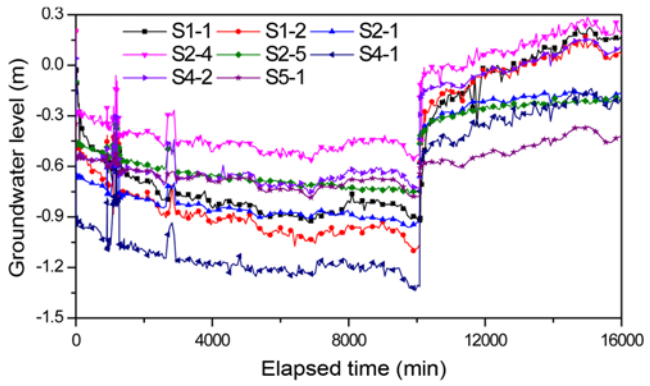

Fig. 6. The Variation of the Groundwater Level in the Monitoring Wells during the Group-Well Pumping Test

After the pump was shut down, the groundwater head recovered quickly. Moreover, the recovery rate of the groundwater head can be divided into two categories. After the pump was shut down, the groundwater head of monitoring wells S1-1, S1-2, S2-4, and S4-2 recovered at higher rates.

2.3.3 Results of Pumping Tests with the Supporting Structure

2.3.3.1 Results of Single-Well Contrast Tests

After the supporting structure within the range of the eastern end of the foundation pit was completed, the supporting structure of the test site was preliminarily closed, after which the contrast tests were carried out. During the excavation of the foundation pit, well S2-5 was damaged by the excavator. Therefore, well S2-4 was chosen as pumping well for subsequent contrast tests. Table 5 reports the results of the single-well pumping contrast tests. The discharge of S2-4 was about 26.0 m^3/h, the drawdown of S2-4 was 13.11 m, and the drawdowns of the monitoring wells were between 0.13 and 0.29 m. Fig. 7 presents the variation of the groundwater level in the monitoring wells during the single-well pumping contrast tests.

Table 5. The Data for the Single-Well Pumping Contrast Tests

Pumping well	Monitoring well	Depth of well screen (m)	Distance from pumping well (m)	Drawdown (m)
S2-4	S2-1	15-23	22.98	0.14
	S2-2	15-23	28.67	0.14
	S2-3	15-23	18.09	0.17
	S2-4	15-23	/	13.11
	S2-5	15-23	11.30	0.29
	S3-1	15-25	22.83	0.14
	S3-2	15-25	20.08	0.13

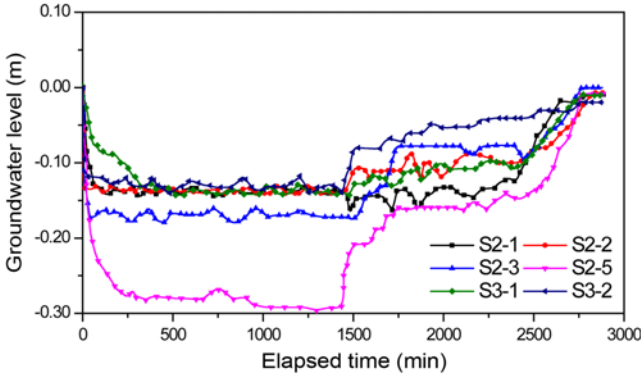

Fig. 7. The Variation of the Groundwater Level in the Monitoring Wells during the Single-Well Pumping Tests

Compared with the groundwater levels in the monitoring wells shown in Fig. 5(a), due to the lengthened groundwater seepage path after the completion of the supporting structure, the declining rate of the groundwater head measured in the monitoring wells was significantly reduced at the beginning of the pumping contrast test. After the pump was shut down, the recovery rate of the groundwater head also decreased. Accordingly, for the case

Table 6. The Data for the Group-Well Pumping Contrast Tests

Label	Depth of well screen (m)	Drawdown (m)		Note
		Contrast test	Pumping test	
S2-2	15-23	13.61	13.93	Dynamic groundwater level inside of the foundation pit
S2-3	15-23	9.26	5.33	Dynamic groundwater level inside of the foundation pit
S3-1	15-25	7.37	15.22	Dynamic groundwater level inside of the foundation pit
S3-2	15-25	11.83	15.59	Dynamic groundwater level inside of the foundation pit
S1-1	5-13	1.51	0.87	Static groundwater level inside of the foundation pit
S1-2	5-13	1.34	1.23	Static groundwater level inside of the foundation pit
S2-1	15-23	1.07	0.84	Static groundwater level inside of the foundation pit
S4-1	24-29	1.05	1.10	Static groundwater level inside of the foundation pit
S4-2	24-29	0.68	0.73	Static groundwater level inside of the foundation pit
S5-1	31-36	0.87	0.34	Static groundwater level inside of the foundation pit
S2-4	15-23	0.49	0.73	Static groundwater level outside of the foundation pit
S2-5	15-23	0.34	0.66	Static groundwater level outside of the foundation pit

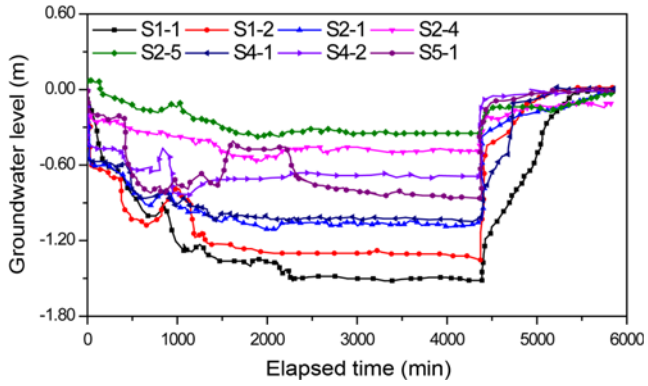

Fig. 8. The Variation of the Groundwater Level in the Monitoring Wells during the Group-Well Pumping Test

in which the pumping rate of S2-4 was only about 26.0 m^3/h, the groundwater level of the pumping well declined sharply to 13.11 m. The results demonstrate that the supporting structure effectively prevented groundwater recharge.

2.3.3.2 Results of the Group-Well Contrast Tests

Table 6 reports the results of the group-well pumping contrast tests. As presented in Tables 2 and 6, when the discharge rate of the pumping wells was unchanged, the drawdown of the groundwater level of the test wells changed significantly. In particular, the groundwater level of monitoring wells, S2-4 and S2-5, which were used to simulate the static groundwater level outside of the foundation pit, declined significantly. Fig. 8 presents the variation of the groundwater levels in the monitoring wells during the group-well pumping contrast test. Compared with the variety of the S2-4 and S2-5 groundwater level measurements shown in Fig. 6, the drawdowns of the static groundwater level outside of the foundation pit were significantly weakened due to the effect of the supporting structure.

Moreover, the drawdown rate of the groundwater level outside of the foundation pit was relatively slow. After the pumps were shut down, the groundwater heads of monitoring wells S1-1 and S4-1 did not recover quickly. Overall, the phenomena exhibited in Fig. 8 indicate that the waterproofing effect of the supporting structure was excellent.

2.3.4 Discussion of the Pumping Tests

The pumping test results demonstrate that the lateral recharge abilities of the unconfined pebble aquifers in the construction site are vital. Taking well S2-5 as an example, to achieve the required reduction in the groundwater level during the construction of the foundation pit, the discharge rate of the pumping well would need to reach 80 m^3/h. Based on the results of the group-well pumping test, when the depth of the well was less than 30 m, the variation of the groundwater level was between 0.84 and 1.10 m, and the changes of each well were consistent. Moreover, the drawdown of the monitoring well at the depth of 37 m was about 0.34 m. Therefore, it can be concluded that the aquifers within the range of the pumping well depth were less affected by the difference between the horizontal and vertical hydraulic conductivities. However, when the buried depth of the aquifers exceeded a specific value, the vertical recharge ability was weakened. Therefore, the reasonable extent of the pumping well for dewatering construction should be greater than 30 m.

As was indicated by the groundwater level variation during the pumping tests, the groundwater head quickly recovered after the pump was shut down. Therefore, during dewatering construction, some standby wells should be set up to ensure construction safety. When completing the construction of the supporting structure, the drawdown of the static groundwater level outside of the foundation pit decreased significantly. The results indicate that the supporting structure played its due role in waterproofing.

3. Analysis of Hydrogeological Parameters

3.1 Neuman Model

As revealed by the pumping test results, the change period of the groundwater level of the monitoring wells can be divided into three stages, an early steep segment, an intermediate flat segment, and a later somewhat steeper segment. Overall, this is a typical characteristic of pumping tests in unconfined aquifers. The unconfined pebble aquifers in Luoyang have layered and anisotropic properties, and are therefore characterized by the combination of flooding sedimentation and overburden pressure. Correspondingly, the difference between the horizontal and vertical hydraulic conductivities in the construction site may be significant. Therefore, to calculate the hydrogeological parameters of unconfined pebble aquifers, a solution method suitable for unconfined, anisotropic aquifers should be employed.

Neuman (1972) developed an analysis method by which to calculate the hydrogeological parameters from pumping tests in an unconfined, anisotropic aquifer. Fig. 9 presents the schematic diagram of the Neuman model. As is commonly known, the Neuman method can be used to obtain the hydrogeological parameters of aquifers for both fully- or partially-penetrating wells. The Neuman model is established based on the following assumptions: the unconfined aquifer is anisotropic and extends laterally indefinitely, the initial surface of the groundwater level is horizontal, and the aquifer flow meets Darcy's law. Then, assuming the unconfined surface as a variable boundary, the following governing equations can be obtained (Neuman, 1972):

$$K_r\left(\frac{\partial^2 s}{\partial r^2}+\frac{1}{r}\frac{\partial s}{\partial r}\right)+K_z\frac{\partial^2 s}{\partial z^2}=S_s\frac{\partial s}{\partial \tau},\ 0<z<H_0, \tag{1}$$

$$s(r,z,0)=0,\ s(\infty,z,t)=0,\ \frac{\partial}{\partial z}s(r,0,t)=0,$$

$$K_z\frac{\partial}{\partial z}s(r,H_0,t)=-\mu\frac{\partial}{\partial t}s(r,H_0,t), \tag{2}$$

$$\lim_{x\to 0}\int_0^{H_0} r\frac{\partial s}{\partial r}\mathrm{d}z=-\frac{Q}{2\pi K_r}, \tag{3}$$

where K_r is the hydraulic conductivity in the horizontal direction (m/

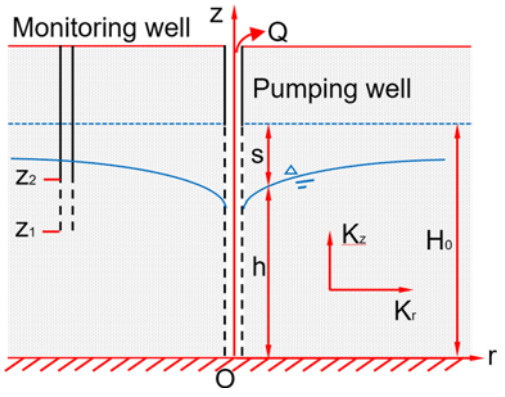

Fig. 9. The Schematic Diagram of the Neuman Model

d), K_z is the hydraulic conductivity in the vertical direction (m/d), S_s is the coefficient of storage (dimensionless), μ is the specific yield of the aquifer (dimensionless), H_0 is the initial saturated thickness of the aquifer (m), s is the drawdown of the free surface at distance r (m), Q is the discharge rate (m^3/d), r is the radial distance from the pumping well (m), and t is the pumping time (d).

For numerical calculation, the following non-dimensional parameters are introduced.

$$\sigma=\frac{S}{\mu},K_d=\frac{K_Z}{K_r},z_d=\frac{z}{H_0},h_d=\frac{H_0}{r},t_s=\frac{Tt}{Sr^2},t_y=\frac{Tt}{\mu r^2},$$
$$\beta=\frac{K_d}{h_d^2}=\frac{r^2K_z}{H_0^2K_r} \quad (4)$$

By applying Laplace and Hankel transforms and inverting the results, the first-order approximation for the original initial-boundary value problem can be obtained. Therefore, the solution of the drawdown is

$$s(r,z,t)=\frac{Q}{4\pi T}\int_0^\infty 4yJ_0(y\beta^{1/2})[\omega_0(y)+\sum_{n=1}^{\infty}\omega_n(y)]\,\mathrm{d}\,y\,, \quad (5)$$

where $\omega_0(y)=\dfrac{\{1-\exp[-t_s\beta(y^2-\gamma_0^2)]\}\cosh(\gamma_0 z_d)}{\{y^2+(1+\sigma)\gamma_0^2-[(y^2-\gamma_0^2)^2/\sigma]\}\cosh(\gamma_0)}$

and $\omega_n(y)=\dfrac{\{1-\exp[-t_s\beta(y^2+\gamma_n^2)]\}\cos(\gamma_n z_d)}{\{y^2-(1+\sigma)\gamma_n^2-[(y^2+\gamma_n^2)^2/\sigma]\}\cos(\gamma_n)}$, in which the terms γ_0 and γ_n are the roots of the following equations,

$$\sigma\gamma_0\sinh(\gamma_0)-(y^2-\gamma_0^2)\cosh(\gamma_0)=0\,,\ \gamma_0^2<y^2\,, \quad (6)$$

$$\sigma\gamma_n\sin(\gamma_n)-(y^2+\gamma_n^2)\cos(\gamma_n)=0\,,\ (2n-1)\frac{\pi}{2}<\gamma_n<n\pi\ (n\geq 1). \quad (7)$$

3.2 Hydraulic Conductivity

3.2.1 Hydraulic Conductivity for Loose to Slightly Dense Pebble Aquifers

From the preceding description of the pumping tests, the filter tube of well S1-1 was located in the loose to slightly dense pebble aquifers. Therefore, based on the discharge rate of well S1-1, and via the use of the data of the groundwater level

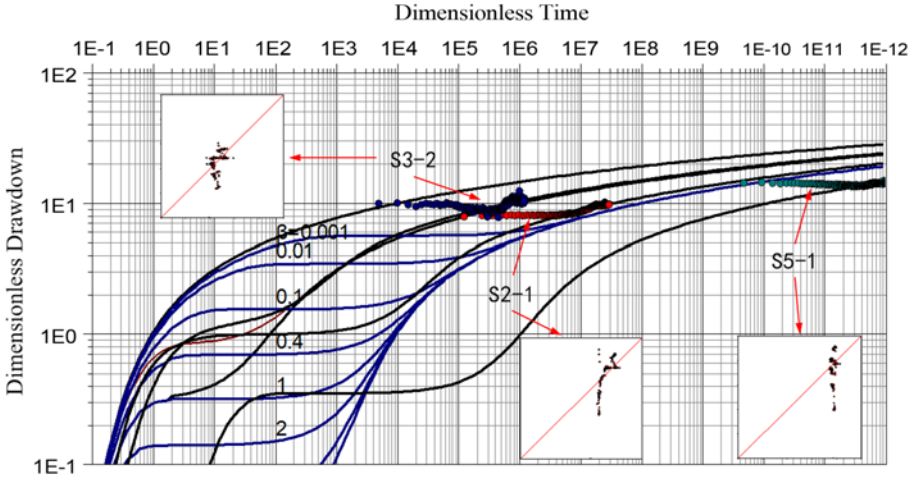

Fig. 10. The Numerical Fitting Curves of the Groundwater Level in the Monitoring Wells (for the loose to slightly dense pebble aquifers)

Table 7. The Hydrogeological Parameters of the Loose to Slightly Dense Pebble Aquifers

Monitoring well	Transmissibility T (m^2/d)	Horizontal hydraulic conductivity K_r (m/d)	Vertical hydraulic conductivity K_z (m/d)	Storage coefficient (Dimensionless)
S2-1	1,230	41	6	4.96×10^{-4}
S3-2	3,080	103	20	1.12×10^{-4}
S4-1	1,070	35.5	7	1.84×10^{-5}
Suggested value	1,800	75	12	2.09×10^{-4}

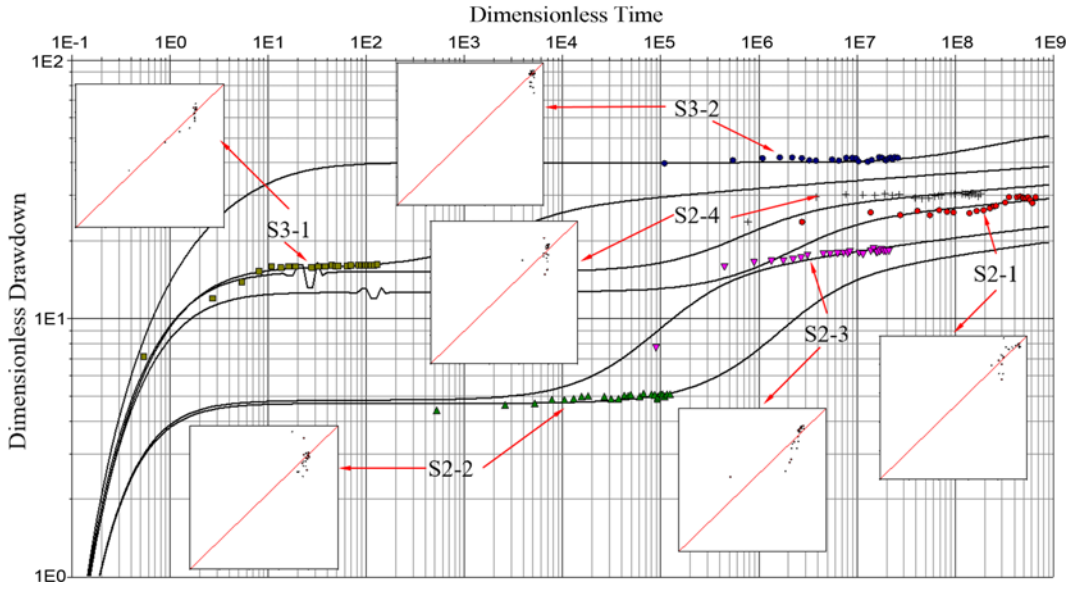

Fig. 11. The Numerical Fitting Curves of the Groundwater Level in the Monitoring Wells (for the medium-dense to compacted pebble aquifers)

Table 8. The Hydraulic Conductivities of the Medium Dense to Compacted Pebble Aquifers

Monitoring well	Horizontal hydraulic conductivity K_r (m/d)		Vertical hydraulic conductivity K_z (m/d)	
	Large drawdown	Small drawdown	Large drawdown	Small drawdown
S1-1	137	104	8	12
S1-2	18.8	59.3	2.5	6.5
S1-3	64.4	110	16	22
S1-4	67.2	98.1	13	20
S2-1	58.2	94	4	8
S2-2	132	82	8	5
Suggested value	79.6	91.2	8.6	12.3

measured in wells S2-1, S3-2, and S5-1, the Neuman model was used to calculate the hydrogeological parameters of the loose to slightly dense pebble aquifers.

Figure 10 presents the fitting results of the drawdown of the groundwater level measured in monitoring wells S2-1, S3-2, and S4-1, and compares the calculated results with the observed values in the form of scatter plots. As shown in the figure, the calculation results are distributed on both sides of the 45-degree contour. Therefore, the hydrogeological parameters obtained by the Neuman model are consistent with the data from the pumping tests. Correspondingly, Table 7 reports the values of the hydrogeological parameters obtained from the Neuman model based on the pumping test data of S1-1. The suggested values of the hydraulic conductivity in the horizontal and vertical directions are 75 and 12 m/d, respectively.

3.2.2 Hydraulic Conductivity for Medium-Dense to Compacted Pebble Aquifers

Using the data of the large-drawdown pumping tests (from 7 a.m. to 7 p.m. on February 22, 2017) and the small-drawdown pumping tests (from 7 p.m. on February 22 to 7 a.m. on February 23, 2017), the numerical fitting of the curves of the decrease of the groundwater level in the monitoring wells over time was carried out. Fig. 11 exhibits the fitting results of the drawdown of the groundwater level measured in monitoring wells S2-1, S2-2, S2-3, S2-4, S3-1, and S3-2 when the pumping well was pumped at a large drawdown. Moreover, the scatter plots compare the differences between the calculated and observed values. As shown in the figure, the hydrogeological parameters calculated by the Neuman model are consistent with the data from the pumping tests. Correspondingly, Table 8 reports the values of the hydraulic conductivity derived from the Neuman model based on the pumping test data of S2-5. The suggested values of the hydraulic conductivity in the horizontal and vertical directions are 86 and 10 m/d, respectively.

4. Numerical Verifications

4.1 Numerical Model

According to the characteristics of the unconfined aquifer and the groundwater boundary conditions of the project, Darcy's law and the principle of continuity were used to establish a three-

dimensional numerical model of the unsteady groundwater flow (Bear, 1979; Johnson et al., 2002; Shen and Xu, 2011; Kuang et al., 2014). The governing equation of the groundwater seepage in saturated media is expressed as follows:

$$\begin{aligned}
&\frac{\partial}{\partial x}\left(k_{xx}\frac{\partial h}{\partial x}\right)+\frac{\partial}{\partial y}\left(k_{yy}\frac{\partial h}{\partial y}\right)+\frac{\partial}{\partial z}\left(k_{zz}\frac{\partial h}{\partial z}\right)-Q=S_s\frac{\partial h}{\partial t} && (x, y, z)\in\Omega\\
&h(x, y, z, t)\big|_{t=0}=h_0\ (x, y, z) && (x, y, z)\in\Omega\\
&h(x, y, z, t)\big|_{\Gamma_1}=h_1\ (x, y, z, t) && (x, y, z)\in\Gamma_1\\
&k_{xx}\frac{\partial h}{\partial n_x}+k_{yy}\frac{\partial h}{\partial n_y}+k_{zz}\frac{\partial h}{\partial n_z}\Big|_{\Gamma_2}=q(x, y, z, t) && (x, y, z)\in\Gamma_1,
\end{aligned} \tag{8}$$

where k_{xx}, k_{yy}, and k_{zz} are the hydraulic conductivities in the main anisotropic directions (m/d), respectively, h (m) is the hydraulic head of point (x, y, z) at time t (d), Q is the source-sink flux, which is a function of the position and time, S_s is the specific storage, $h_0(x, y, z)$ (m) is the initial hydraulic head at point (x, y, z), Γ_1 and Γ_2 are the first and second types of boundary conditions, respectively, $h_1(x, y, z)$ (m) is the constant head on the boundary Γ_1, n_x, n_y, and n_z are the unit normal vectors on the boundary Γ_2 along the x, y, and z directions, respectively, $q(x, y, z, t)$ (m^3/d) is the lateral recharge per unit area on the boundary Γ_2, and Ω is the computational domain.

4.2 Calculation Range

The numerical simulation range was determined according to the geotechnical survey report, hydrogeological conditions, and drilling data,. based on the following principles. With the pumping test area as the center and the extension of the boundary of the numerical simulation range to the outside of the influence radius of the pumping wells, the entire area of in-plane calculation was 4,000 × 4,260 m. Correspondingly, the engineering geology includes five strata, from top to bottom, it is divided into a loose to slightly dense pebble stratum (7.0 – 13.5 m), a medium-dense to compacted pebble stratum (13.5 – 24.0 m), another medium-dense to compacted pebble stratum (24.0 – 30.0 m), a compacted pebble stratum (30.0 – 37.0 m), and another compacted pebble stratum (37.0 – 100.0 m). Fig. 12 presents the schematic diagram of the three-dimensional (3D) finite element model. As shown in Fig. 12(b), the meshes are most densely located in the test site, and gradually become sparse with the increase of the distance from the test site.

4.2.1 Hydraulic Characteristics of Unconfined Pebble Aquifers

The unconfined pebble aquifers in the construction site are widely distributed and thick, and the groundwater movement conforms to Darcy's law. Because there is transparent flow exchange and a vertical interlayer overflows between the aquifer

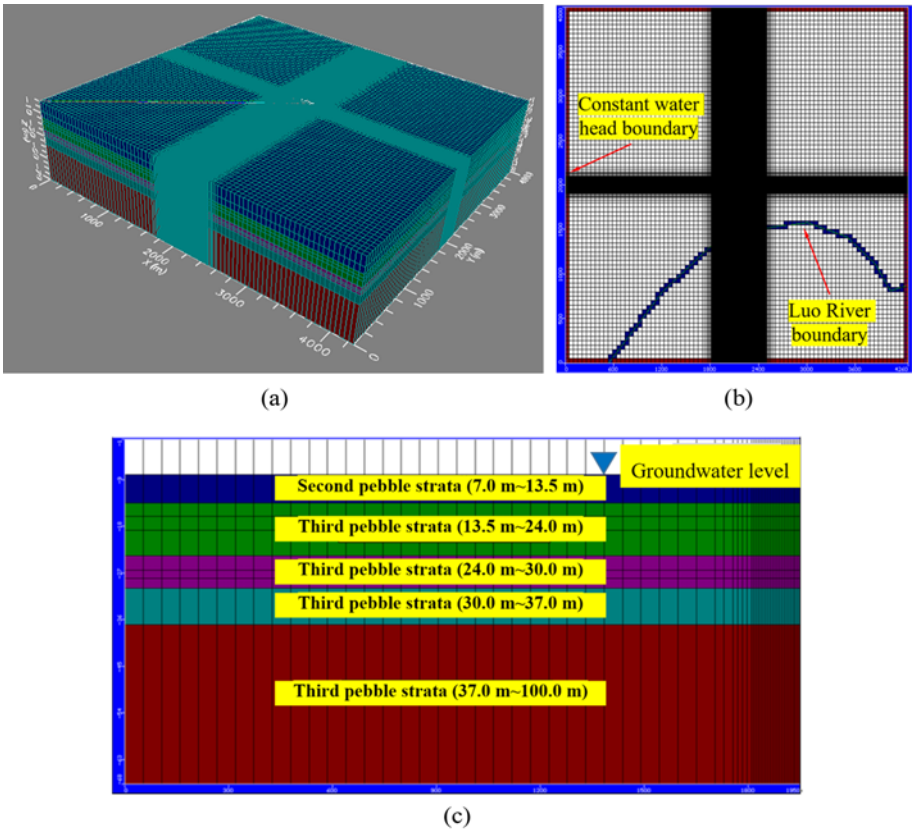

Fig. 12. Schematic Diagram of the Finite Element Model: (a) 3D Finite Element Mesh, (b) In-Plane Analysis Range and Mesh, (c) Profile of the Generalized Pebble Aquifer Distribution

layers, the groundwater movement can be generalized into a 3D spatial flow. Furthermore, the groundwater flow system conforms to the laws of mass and energy conservation. Considering the heterogeneous characteristics of the unconfined pebble aquifer, the input and output of the groundwater seepage system changed with time and space in the finite element analysis. Moreover, with spatial variations, the aquifers can be generalized into the horizontal, isotropic medium. Therefore, a 3D unsteady groundwater seepage system within a heterogeneous and horizontal isotropic medium was established for the simulation range.

4.2.2 Pumping Wells and Boundary Conditions

Based on the structure of the test well, the parameters of the pumping wells, such as the filter tube length and discharge rate, were set in the finite element model. The positions and structures of the test wells were set with reference to Figs. 3 and 4. According to the observations of the test site, the boundaries in the finite element model were set as the constant water head boundary and river recharge boundary, as presented in Fig. 12. Moreover, the water levels of the boundaries remained unchanged and were set outside the range affected by the pumping tests.

4.2.3 Back-Calculation Process

The parameters of the unconfined pebble aquifers were inverted to calculate their hydrogeological parameters via trial-and-error adjustment (Mark and Kich, 2002). In the back-calculation process, the inversion of the hydraulic conductivity of each aquifer was carried out by a combination of manual adjustment and automatic program optimization. First, based on the data of the single-well pumping test of S2-5, the pebble aquifer parameters were searched and inverted to obtain the hydrogeological parameters with the best fit with the test data. Then, the obtained hydrogeological parameters were identified and verified using the data from the group-well pumping test. Finally, a two-well pumping verification test in the construction site was employed to correct the parameters of the numerical model and verify the credibility of the model. Moreover, the numerical model can be used to design and analyze dewatering construction.

4.3 Simulation Results

4.3.1 Parameter Identification

Figure 13 presents the comparison between the observed data and the calculated groundwater head of the measurement holes during the single-well pumping test of S2-5. To facilitate the analysis, the data of the pore water pressure gauges in measurement holes KS1, KS3, and KS4 were selected as the on-site observed values. Fig. 13 reveals that the observed data corresponding to points A and B were the pore water pressure values at different buried depths. Overall, the calculated results were found to match the observed results for most of the measurement holes. The numerical results demonstrate that the values obtained from the single-well pumping test truly reflect the hydrogeological characteristics of the unconfined pebble aquifers.

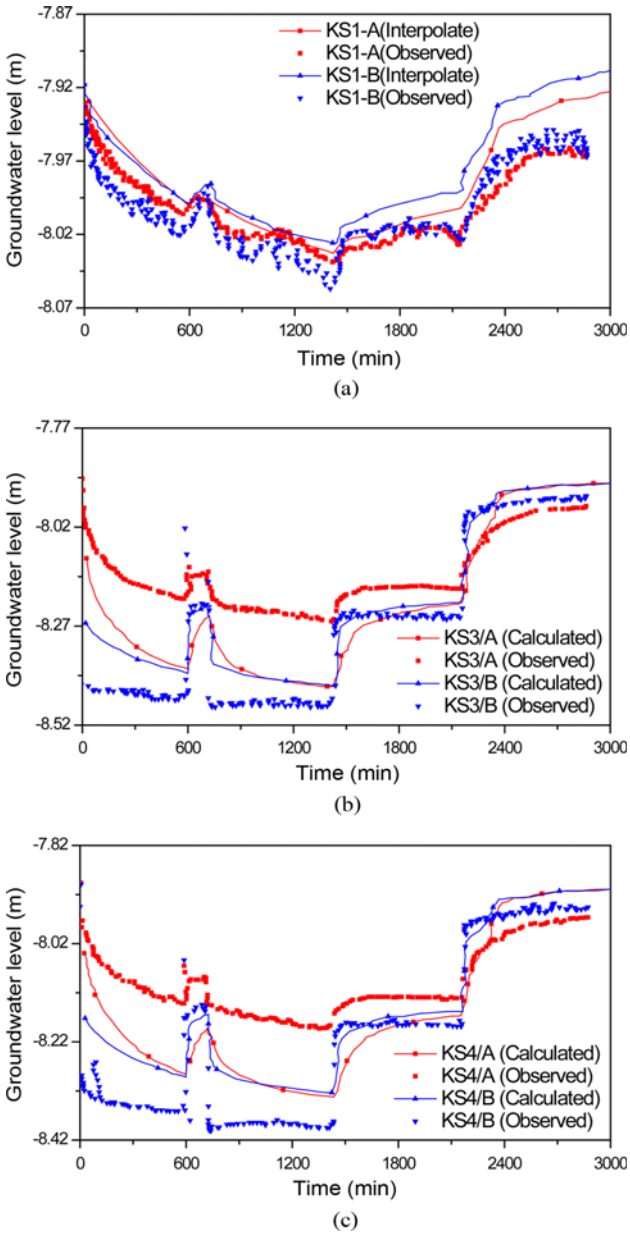

Fig. 13. The Comparison between the Observed and Calculated Groundwater Head during the Single-Well Pumping Test of S2-5: (a) KS1, (b) KS3, (c) KS4

The group-well pumping test before the supporting structure was finished was used as a simulation prototype, and the data of the groundwater head were used as the appropriate benchmarks. The hydrogeological parameters of the unconfined pebble aquifers were determined according to the observed data of the meansurement holes. Fig. 14 presents the comparison between the observed data and the calculated groundwater head of the measurement holes during the group-well pumping test. As revealed by the figure, the calculated results mathed the observed data of measurement hole KS2.

Via the reliability analysis using the data of the single-well and group-well pumping tests to fit and adjust the hydrogeological

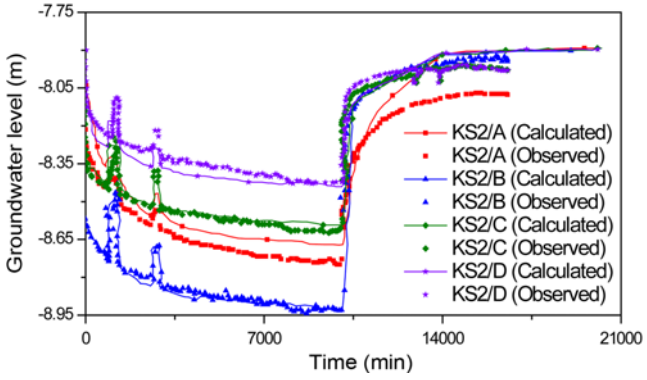

Fig. 14. The Comparison between the Observed and Calculated Groundwater Heads in KS2 during the Group-Well Pumping Test

Table 9. The Calculation Results of the Hydraulic Conductivities of Each Pebble Aquifer

Aquifer	Horizontal hydraulic conductivity K_r (m/d)	Vertical hydraulic conductivity K_z (m/d)
Second pebble strata (7.0 – 13.5 m)	70	10
Third pebble strata (13.5 – 24.0 m)	80	10
Third pebble strata (24.0 – 30.0 m)	85	12
Third pebble strata (30.0 – 37.0 m)	100	15
Third pebble strata (37.0 – 70.0 m)	100	15

parameters of the unconfined pebble aquifers, the calculated parameters were found to be within the 95% confidence interval. Thus, the fitting results of the hydrogeological parameters are reliable. Table 9 reports the calculation results of the hydraulic conductivities of each pebble aquifer in the numerical model.

4.3.2 Numerical Model Calibration

To further verify the reliability of the numerical model and the hydrogeological parameters of the unconfined pebble aquifers, a two-well pumping verification test was carried out on August 3, 2017. The verification test was arranged after the construction of the dewatering wells had been completed halfway. Fig. 15 presents the schematic diagram of the two-well pumping verification test and the layout of the pumping and monitoring wells; S2 and S24 were the pumping wells, and S23 and G44 were the monitoring wells.

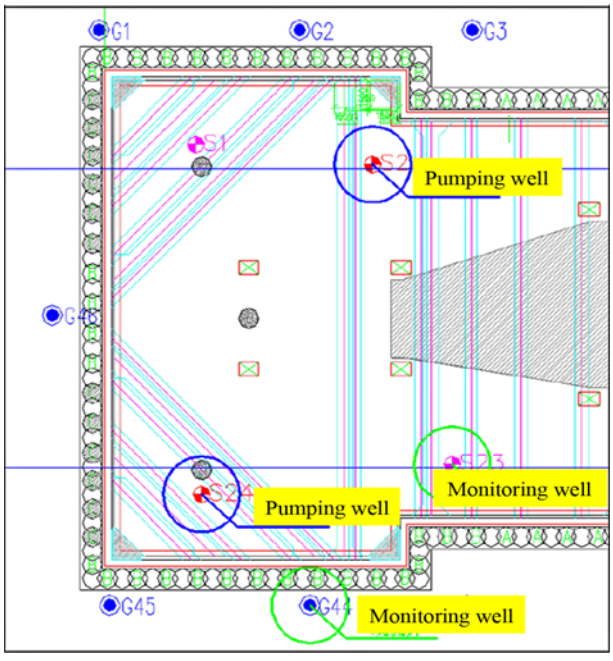

Fig. 15. The Schematic Diagram of the Two-Well Pumping Verification Test

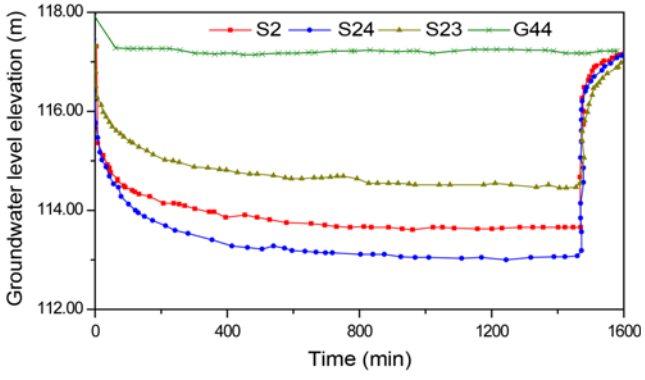

Fig. 16. The Variation of the Groundwater Level Measured in the Test Wells during the Two-Well Pumping Verification Test

During the two-well pumping verification test, the discharge of S2 was about 79.83 m^3/h, and its drawdown was 10.78 m. The discharge of S24 was approximately 83.87 m^3/h, and its drawdown was 11.43 m. The depths of the static groundwater heads of monitoring wells S23 and G44 was 9.95 and 8.01 m, respectively. Table 10 reports the results of the two-well pumping verification test, and Fig. 16 presents the variation of the measured dynamic

Table 10. The Data of the Two-Well Pumping Verification Test

Label	Elevation of well (m)	Depth of initial groundwater level (m)	Elevation of initial groundwater level (m)	Depth of groundwater level after pumping (m)	s_w (m)	Q (m^3/h)
S2	+124.481	7.10	+117.381	10.78	3.68	79.83
S24	+124.511	7.10	+117.411	11.43	4.33	83.87
S23	+124.510	7.15	+117.360	9.95	2.80	/
G44	+125.197	7.27	+117.927	8.01	0.74	/

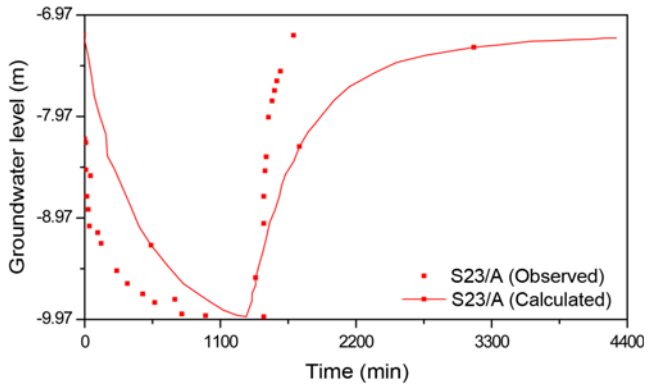

Fig. 17. The Comparison between the Observed and Calculated Groundwater Heads Measured in Monitoring Well S23 during the Two-Well Pumping Verification Test

Table 11. The Hydraulic Conductivities of the Unconfined Pebble Aquifers

Aquifer	Horizontal hydraulic conductivity K_r (m/d)	Vertical hydraulic conductivity K_z (m/d)
Second pebble strata	75	10
Third pebble strata	90	15

groundwater levels. The data from the two-well pumping verification test were substituted into the 3D numerical model to verify the hydrogeological parameters of the unconfined pebble aquifers exhibited in Table 9. Fig. 17 presents the comparison between the observed data and the calculated groundwater head of monitoring well S23. As shown in the figure, the calculated results were found to math the observed data for monitoring well S23. For simplicity, Table 11 provides the suggested values of the hydraulic conductivities of the unconfined pebble aquifers for dewatering construction design.

5. Conclusions

This paper reported the results of pumping tests in Shijiawan station, Luoyang City, China to investigate the hydrogeological characteristics of unconfined pebble aquifers. Based on the data from the pumping tests, the hydraulic conductivities of the unconfined pebble aquifers were obtained by the analytical method and numerical simulation. The results of the pumping tests and the analysis of the present case study yield the following conclusions.

1. There is an apparent vertical water recharge between the unconfined pebble aquifers. Considering that the vertical recharge capacity is weakened when the aquifer's thickness is too large, it is recommended that the depth of the pumping well in the dewatering construction be more than 30 m.
2. The values of the hydraulic conductivities of the aquifers were calculated using the Neuman method. For the loose to slightly dense pebble aquifers, the suggested values of the hydraulic conductivities in the horizontal and vertical directions are 75 and 12 m/d, respectively. For the medium-dense to compacted pebble aquifers, these values are respectively 86 and 10 m/d.
3. A three-dimensional numerical model for the simulation of pumping tests was established. Based on data from actual pumping tests, the values of the horizontal and vertical hydraulic conductivities were obtained by back-calculation. Compared with the analytical method, the numerical method can indicate the hydrogeological characteristics of other aquifers in the construction site.
4. The supporting structure plays a useful role in waterproofing. When the discharge of pumping wells is similar, the dynamic groundwater level of the monitoring wells outside the supporting structure is significantly reduced.
5. In the future evaluation of the hydrogeological parameters of unconfined pebble aquifers, it is necessary to explore the application of the results to the dewatering design of the foundation pits of metro stations. Moreover, the research results would provide an effective method for the evaluation of the hydrogeological parameters of similar unconfined aquifers.

Acknowledgments

The authors gratefully acknowledge the financial support provided by the National Natural Science Foundation of China (Grant no. 11502072). The authors are grateful for the funds provided by Luoyang Rail Transit Co. Ltd. (Grant no. LYGD1-ZX-HYFW-(2017)118-chlscky). The authors also thank the Young-backbone Teacher Foundation of Colleges and Universities of Henan Province (Grant no. 2019GGJS076).

ORCID

Jianjun Ma https://orcid.org/0000-0003-1594-6950

References

Bear J (1979) Hydraulics of groundwater. McGraw-Hill, New York, NY, USA, 60-72

Cao C, Shi C, Liu L, Liu J, Lei M, Lin Y, Ye Y (2019) Novel excavation and construction method for a deep shaft excavation in ultrathick aquifers. *Advances in Civil Engineering* 2019:1827479, DOI: 10.1155/2019/1827479

Chapuis RP (1992) Similarity of internal stability criteria for granular soils. *Canadian Geotechnical Journal* 29(4):711-713, DOI: 10.1139/t92-078

Chapuis RP (2004) Predicting the saturated hydraulic conductivity of sand and gravel using effective diameter and void ratio. *Canadian Geotechnical Journal* 41(5):787-795, DOI: 10.1139/t04-022

Chapuis RP, Dallaire V, Marcotte D, Chouteau M, Acevedo N, Gagnon F (2005) Evaluating the hydraulic conductivity at three different scales within an unconfined sand aquifer at Lachenaie, Quebec. *Canadian Geotechnical Journal* 42(4):1212-1220, DOI: 10.1139/

t05-045
Çimen M (2008) Confined aquifer parameters evaluation by slope-matching method. *Journal of Hydrologic Engineering* 13(3):141-145, DOI: 10.1061/(ASCE)1084-0699(2008)13:3(141)
GB50027-2001 (2001) Standard for hydrogeological investigation of water-supply. GB50027-2001, China Architecture & Building Press, Beijing, China (in Chinese)
GB50296-2014 (2014) Technical code for tube well. GB50296-2014, China Planning Press, Beijing, China (in Chinese)
Huang H, Qian J (2012) Experimental study of airflow induced by pumping tests in unconfined aquifer with low-permeability cap. *Journal of Hydrodynamics* 24(4):605-608, DOI: 10.1016/S1001-6058(11)60283-7
Jean JS (1996) Pumping testing using a siphon well. *Water Resources Management* 10(2):81-105, DOI: 10.1007/BF00429681
Jiao J (1996) Investigation of possible extra recharge during pumping in Nottingham aquifer. *Groundwater* 34(5):795-800, DOI: 10.1111/j.1745-6584.1996.tb02073.x
Johnson GS, Frederick DB, Cosgrove DM (2002) Evaluation of a pumping test of the Snake River Plain aquifer using axial-flow numerical modelling. *Hydrogeology Journal* 10(3):428-437, DOI: 10.1007/s10040-002-0201-0
Kuang X, Jian JJ, Zhang K, Mao D (2014) Air and water flows induced by pumping tests in unconfined aquifers with low-permeability zones. *Hydrological Processes* 28(21):5450-5456, DOI: 10.1002/hyp.10058
Lin HT, Tan YC, Chen CH, Yu HL, Wu SC, Ke KY (2010) Estimation of effective hydrogeological parameters in heterogeneous and anisotropic aquifers. *Journal of Hydrology* 389(1-2):57-68, DOI: 10.1016/j.jhydrol.2010.05.021
Ma L, Xu Y, Shen S, Sun W (2014) Evaluation of the hydraulic conductivity of aquifers with piles. *Hydrogeology Journal* 22(2):371-382, DOI: 10.1007/s10040-013-1068-y
Mark B, Kick H (2002) A Dupuit formulation for flow in layered, anisotropic aquifers. *Advances in Water Resources* 25(7):747-754, DOI: 10.1016/S0309-1708(02)00074-X
Neuman SP (1972) Theory of flow in unconfined aquifers considering delayed response of the water table. *Water Resources Research* 8(4):1031-1045, DOI: 10.1029/WR008i004p01031
Neuman SP, Blattstein A, Riva M, Tartakovsky DM (2007) Type curve interpretation of late-time pumping test data in randomly heterogeneous aquifers. *Water Resources Research* 43(10):1-15, DOI: 10.1029/2007WR005871
Ou CY, Chen SH (2010) Performance and analysis of pumping tests in a gravel formation. *Bulletin of Engineering Geology and the Environment* 69(1):1-12, DOI: 10.1007/s10064-009-0218-x
Sethi R (2011) A dual-well step drawdown method for the estimation of linear and non-linear flow parameters and wellbore skin factor in confined aquifer systems. *Journal of Hydrology* 400(1-2):187-194, DOI: 10.1016/j.jhydrol.2011.01.043
Shaqour FM, Hasan SE (2008) Groundwater control for construction purposes: A case study from Kuwait. *Environmental Geology* 53(8):1603-1612, DOI: 10.1007/s00254-007-0768-9
Shen SL, Xu YS (2011) Numerical evaluation of land subsidence induced by groundwater pumping in Shanghai. *Canadian Geotechnical Journal* 48(9):1378-1392, DOI: 10.1007/s12204-013-1394-1
Shen S, Wu Y, Xu Y, Hion T, Wu H (2015) Evaluation of hydraulic parameters from pumping tests in multi-aquifers with vertical leakage in Tianjin. *Computers and Geotechnics* 68:196-207, DOI: 10.1016/j.compgeo.2015.03.011
Wu SC, Tan YC, Chen CH, Lin ST, Ke KY (2008) A two-dimensional inverse model to identify transmissivity in an anisotropic aquifer. *Hydrological Processes* 22(26):5086-5096, DOI: 10.1002/hyp.7134
Yeh H, Huang Y (2009) Analysis of pumping test data for determining unconfined-aquifer parameters: Composite analysis or not? *Hydrogeology Journal* 17:1133-1147, DOI: 10.1007/s10040-008-0413-z
Zhang L, Zhou X, Pan Y, Zeng B, Zhu D, Jiang H (2020) Design of groundwater extraction in open cut foundation pit and simplified calculation of ground subsidence due to dewatering in sandy pebble soil strata. *Advances in Civil Engineering* 2020:1046937, DOI: 10.1155/2020/1046937